TECHNICAL TRANSACTIONS | **CZASOPISMO TECHNICZNE**
ELECTRICAL ENGINEERING | ELEKTROTECHNIKA
2-E/2015

ANDRZEJ SZROMBA*

CONDUCTANCE CONTROL OF A SHUNT ACTIVE POWER FILTER AND ACTIVE ENERGY BUFFER

ENERGOELEKTRONICZNY FILTR AKTYWNY I BUFOR ENERGII AKTYWNEJ STEROWANY KONDUKTANCYJNIE

A b s t r a c t

There are many types of control method for shunt active power filter (SAPF) investigated up until now. The authors describe complex methods of determining active filter reference currents or powers. This paper is dedicated to a simple, but universally used control algorithm based on the load equivalent conductance approach. This method allows for non-active current compensation, energy buffering, and energy redistribution among loads under compensation. It is also useful for voltage-source as current--source inverter based active filters, and for DC system as well as for AC single or three-phase filters.

Keywords: *active filter*, *active current*, *load equivalent conductance*, *indirect current control*, *energy buffering*, *harmonics and interharmonics*

S t r e s z c z e n i e

Zadaniem energoelektronicznego filtru aktywnego jest kompensacja prądu nieaktywnego w gałęzi źródła zasilania. Znanych jest wiele metod pozyskiwania informacji niezbędnych do skompensowania tego prądu. Często są to wyrafinowane metody, bardzo złożone zarówno pod względem pojęciowym, jak i obliczeniowym. W niniejszym artykule przedstawiono nieskomplikowaną, lecz wydajną i wielofunkcyjną metodę uzyskiwania wzorca składowej czynnej prądu obciążenia. Jest ona oparta na pojęciu konduktancji zastępczej obciążenia. Umożliwia nie tylko kompensację prądu nieaktywnego, ale również sterowanie przepływem energii czynnej, w tym jej rekuperację i redystrybucję do kompensowanych obciążeń. Opisana metoda może być stosowana w obwodach jedno- i wielofazowych, a także w obwodach zasilanych sygnałem stałym. Może też zostać użyta wobec filtru aktywnego opartego i na falowniku napięcia, i na falowniku prądu.

Słowa kluczowe: *energoelektroniczny filtr aktywny*, *prąd aktywny*, *konduktancja zastępcza*, *buforowanie i redystrybucja energii*, *harmoniczne*

DOI: 10.4467/2353737XCT.15.092.3924

* Ph.D. Eng. Andrzej Szromba, Faculty of Electrical and Computer Engineering, Cracow University of Technology.

1. Introduction

In general, the SAPF control techniques may be classified as based upon either undesirable or desirable components of load current (or power). When focusing on undesirable components (Fig. 1), the load current waveform is analysed to compute specific attributes of its distortion. The distortion is characterised by harmonic components (their amplitudes, frequencies and phases), more and more often also including a DC component, interharmonics and subharmonics, fluctuations of harmonics amplitudes and even noise – which may be handled separately due to differences in measurement techniques and outcomes. These components are then used as the reference for filtering the current forming. This technique is often referred to as the open-loop control method. It is supposed to be flexible by means of choosing components to be compensated. Such control strategy utilizes versatile and complex types of harmonic current extraction, using either frequency-domain or time-domain methods: various types of Fourier transform; wavelet transform; Clark/Park direct and inverse transformation; signal filtration etc. The dynamic performance of an active filter mainly depends on how exactly and how quickly the harmonic components are extracted from the load current. Scientists and engineers debate the accuracy of various methods of harmonic detection, its dynamics and stability, ease and cost of implementations, etc.

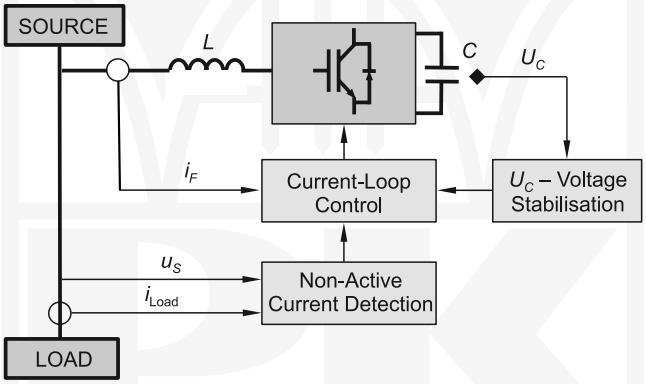

Fig. 1. Non-active current based control of SAPF

Using the principle ‘keep it as simple as possible’, the active current based control strategy may be focused on only one load current component – on its active component, Fig. 2. The active component has to be sinusoidal, in-phase with the source voltage and balanced in the case of a three-phase system. It is now clear that the only quantity to obtain is the amplitude of a sine wave signal, this is much easier than calculating the numbers of harmonic/interharmonic/subharmonic attributes. Finally, having the active component amplitude, the active filter controls the source current to be equal to the active component of the load current.

This technique is often referred to as the closed-loop control or the global compensation. Voltage and current signals are mostly used to determine the load active current [1–11], this is known as the direct current control method.

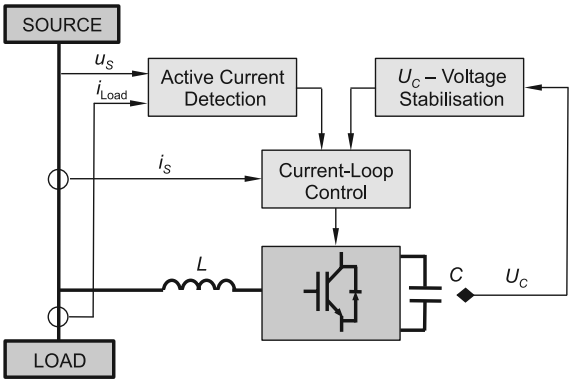

Fig. 2. Active current based control of SAPF

Alternatively, the active current based control strategy may be implemented using the indirect control method [2, 12–30]. Then, the active current is determined on the basis of energy stored in the filter's capacitor *C* and reactor *L*. Such technique are developed in this paper. The base structure of the considered active filter is shown in Fig. 3.

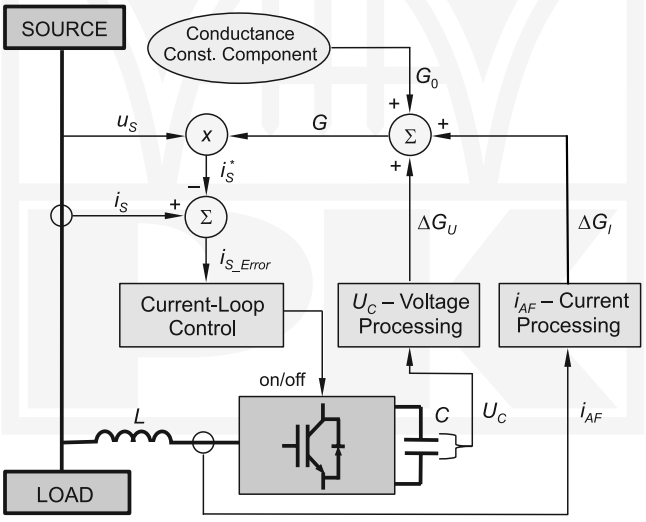

Fig. 3. The indirectly controlled SAPF considered in this paper

This paper describes a concept and then the simulation analysis of the conductance controlled SAPF with the capability of active energy flow control.

Fryze's idea of load equivalent conductance is employed in this paper. This conductance is related to the load active power. It may be positive or negative – dependent upon the direction of the active energy flow. Using this conductance, the reference signal for the source current can be determined. No harmonic extraction is needed, hence computational

effort of the filter's control module may be significantly reduced. Such a control technique allows the shaping of the source current to be strictly active and enables buffering the flow of the active energy.

2. In-circuit energy relations

For energy delivering, the active current is necessary and the non-active current is unwanted. This is in good agreement with Fryze's active current idea [31].

The active power P for the n-th period T is defined as:

$$P_{nT} = \frac{1}{T} \int_{(n-1)T}^{nT} u_S i_S dt \tag{1}$$

$n = 1, 2, 3, \ldots$; u_S, i_S are the source voltage and the current.

Power P_{nT} is the sum of the powers of all circuit components supplied by the source, including the active filter. Within each period T, the active power (1) may be considered as the sum of a constant predefined component P_0 and variable component ΔP_{nT}:

$$P_{nT} = P_0 + \Delta P_{nT} \tag{2}$$

Then, the Fryze's equivalent conductance for the n-th period T may be determined:

$$G_{nT} = \frac{P_{nT}}{U_S^2} \tag{3}$$

$$G_{nT} = \frac{P_0 + \Delta P_{nT}}{U_S^2} = G_0 + \Delta G_{nT} \tag{4}$$

where:

$$G_0 = \frac{P_0}{U_S^2} \quad \text{(see Fig. 3)} \tag{5}$$

and

$$\Delta G_{nT} = \frac{\Delta P_{nT}}{U_S^2} = \frac{P_{nT} - P_0}{U_S^2} \tag{6}$$

The conductance variable component (6) can only be known if the active power (1) is already obtained. The whole time period T is needed to calculate this power, so the information on the magnitude of the component ΔG is always delayed for one period T:

$$G_{nT} = \frac{P_0 + \Delta P_{(n-1)T}}{U_S^2} = G_0 + \Delta G_{(n-1)T} \tag{7}$$

The conductance (7) is then used to produce the source current reference signal $i_{S,nT}^*$:

$$i_{S,nT}^* = (G_0 + \Delta G_{(n-1)T})\, u_S \tag{8}$$

Due to maintaining constant magnitude of the equivalent conductance within each period T, the source current may be pure sinusoidal if the source voltage signal u_S is provided as non-distorted [9, 32].

The definition (1) requires measuring the load voltage and current. However, in this paper, the load active power is determined indirectly on the basis of energy stored in the filter's reactance elements C and L. The filter's energy change during period T_1 is:

$$\Delta W_{1T,AF} = (P_0 - P_{1T})T \tag{9}$$

where $\Delta W_{1T,AF}$ is the change of energy stored in the filter's capacitor C and inductor L.

Let the instantaneous energy stored in the capacitor be denoted as w^{DC} and the inductor's energy as w^{AC} (on the DC-side and AC-side of the filter, respectively). Initial energy is denoted as W^{DC} and W^{AC}, respectively. The after n periods T change of filter energy is:

$$\begin{aligned}
\Delta W_{AF} &= \left[(W_0^{DC} + W_0^{AC}) - (w_{1T}^{DC} + w_{1T}^{AC})\right] + \left[(w_{1T}^{DC} + w_{1T}^{AC}) - (w_{2T}^{DC} + w_{2T}^{AC})\right] + \cdots + \\
&+ \left[(w_{(n-2)T}^{DC} + w_{(n-2)T}^{AC}) - (w_{(n-1)T}^{DC} + w_{(n-1)T}^{AC})\right] + \left[(w_{(n-1)T}^{DC} + w_{(n-1)T}^{AC}) - (w_{nT}^{DC} + w_{nT}^{AC})\right] = \\
&= W_0^{DC} + W_0^{AC} - w_{1T}^{DC} - w_{1T}^{AC} + w_{1T}^{DC} + w_{1T}^{AC} - w_{2T}^{DC} - w_{2T}^{AC} + \cdots + \\
&+ w_{(n-2)T}^{DC} + w_{(n-2)T}^{AC} - w_{(n-1)T}^{DC} - w_{(n-1)T}^{AC} + w_{(n-1)T}^{DC} + w_{(n-1)T}^{AC} - w_{nT}^{DC} - w_{nT}^{AC} = \\
&= (W_0^{DC} - w_{nT}^{DC}) + (W_0^{AC} - w_{nT}^{AC})
\end{aligned} \tag{10}$$

Finally, the filter energy change ΔW_{AF} may be described as:

$$\Delta W_{AF} = \sum_{1}^{n} \Delta P_{nT} T = \frac{C(U_{C0}^2 - U_{C,nT}^2) + L(I_{AF0}^2 - I_{AF,nT}^2)}{2} \tag{11}$$

where:

- C – the capacity of the filter's capacitor,
- U_{C0} – the capacitor's initial voltage,
- $U_{C,nT}$ – the capacitor's voltage at the end of the n-th period T,
- L – the filter's inductor,
- I_{AF0} – the filter's initial current,
- $I_{AF,nT}$ – the filter's current at the end of n-th period.

3. Filter's control structure

Using (8) and (11), the reference current is:

$$i_{S,nT}^{*} = \left[G_0 + \frac{C(U_{C0}^2 - U_{C,(n-1)T}^2) + L(I_{AF0}^2 - I_{AF,(n-1)T}^2}{2TU_S^2} \right] u_s \tag{12}$$

The control structure diagram corresponding with the formula (12) is shown in Fig. 4. In the Figure 4, the one T period time delay effect (7), is executed using *sync* and *S/H* modules. The *sync* module generates synchronization pulses at the end of each period T. The *S/H* module is a sample-and-hold device.

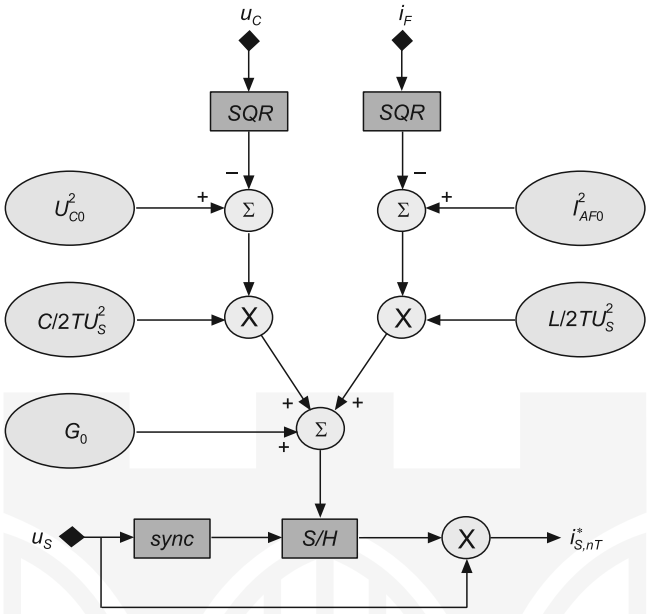

Fig. 4. Filter's control structure on the base of formula (12)

There are possibilities for reducing the complexity of the formula (13) and the control structure shown in Fig. 4:

a) by neglecting filter initial current. The filter's initial current I_{AF0} (at the instant of filter turn-on) is null, therefore the filter initial current I_{AF0}^2 in (12) may be zeroed, so:

$$i_{S,nT}^* = \left[G_0 + \frac{C(U_{C0}^2 - U_{C,(n-1)T}^2) - LI_{AF,(n-1)T}^2}{2TU_S^2} \right] u_s \tag{13}$$

b) by neglecting the filter's inductor energy. The initial magnitude of the filter's capacitor voltage U_{C0} is significantly higher then the peak $U_{S\max}$ of the supply source voltage, for example $U_{C0} \cong 1.5U_{S\max}$. Changes of the capacitor voltage may be presupposed to be about $\pm 0.1U_{C0}$. Taking the capacitor's capacity and voltage to be 4 mF and 500 V respectively, the initial capacitor's energy is 500 J and the capacitor's energy variation is 100 J. Taking the inductor's inductance to be 5 mH and presupposing the inductor's peak current 15 A, the inductor's energy variation is 0.6 J. Therefore the conductance variable component may be obtained only as a function of the filter's capacitor voltage:

$$i_{S,nT}^* = \left[G_0 + \frac{C(U_{C0}^2 - U_{C,(n-1)T}^2)}{2TU_S^2} \right] u_s \tag{14}$$

Disregarding the filter's inductor energy may cause insignificant alterations of the variable component (6).

c) by substituting U_C for U_C^2. The simplified conductance variable component ΔG_{nT} introduced in (14) is:

$$\frac{C(U_{C0}^2 - U_{C,(n-1)T}^2)}{2TU_S^2} \tag{15}$$

this may be rewritten as:

$$\alpha_{U\wedge 2}(U_{C0}^2 - U_{C,(n-1)T}^2), \quad \text{where} \quad \alpha_{U\wedge 2} = \frac{C}{2TU_S^2} \tag{16}$$

For capacitor voltages U_{C0} = 500 V, $U_{C\max}$ = 520 V and $U_{C\min}$ = 480 V, the component (16) may be replaced by:

$$\alpha_{U\wedge 1}(U_{C0} - U_{C,(n-1)T}), \quad \text{with} \quad \alpha_{U\wedge 1} = 1.95 \cdot 10^{-3} \tag{17}$$

this sufficiently linearises equation (14). Finally, the reference current is:

$$i_{S,nT}^* = \left[G_0 + \alpha_{U\wedge 1}(U_{C0} - U_{C,(n-1)T}) \right] u_s \tag{18}$$

The diagram of the filter's control structure corresponding with formula (18) is shown in Fig. 5. This structure is simpler when compared with the structure shown in Fig. 4.

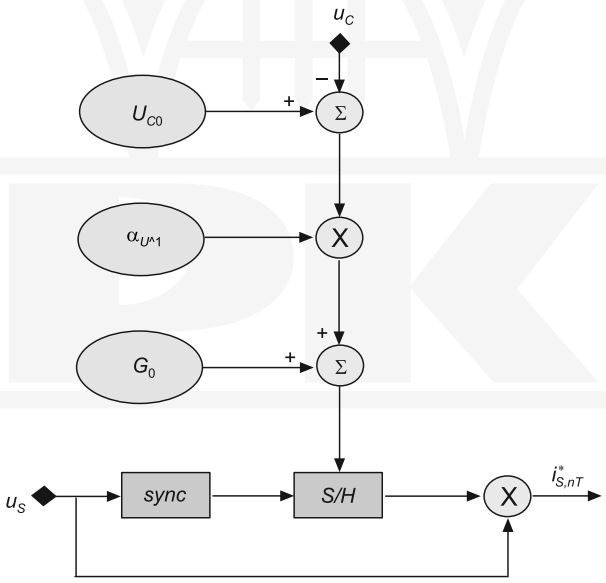

Fig. 5. Filter's control structure on the base of formula (18)

4. Simulations

Simulations shown in this section verify the main feature of the considered filter working in a single-phase circuit. All waveforms are obtained using the Intusoft ICAP software. Parameters of the simulated circuit are as follows:

- Source: $U_S = 230$ V, $R_S = 50$ mΩ, $L_S = 100$ μH.
- Load: time-dependent resistor, $R = 0$ for each 1st and 3rd quarter of each period T, and $R = 20$ Ω for each 2nd and 4th quarter of each period T.
- Conductance constant component $G_0 = 43.5$ mS.
- Filter's reactance elements $C = 4$ mF and $L = 5$ mH.

Figures 6 and 7 show essential signals in the circuit. Equation (18) and the filter structure depicted in Figs. 3 and 5 are used. The period-table detailed filter action.

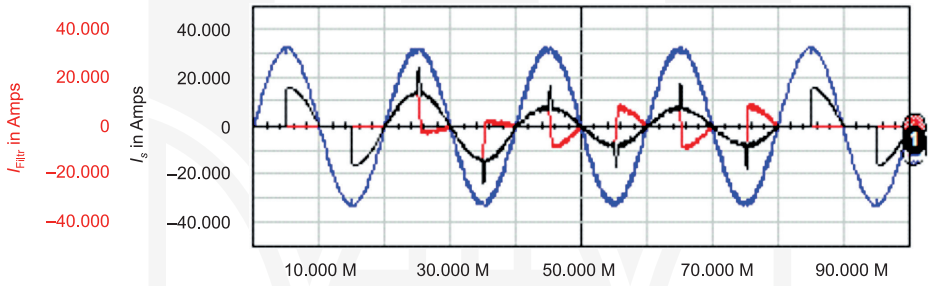

Fig. 6. Source voltage (blue), filter current (red) and source current (black)

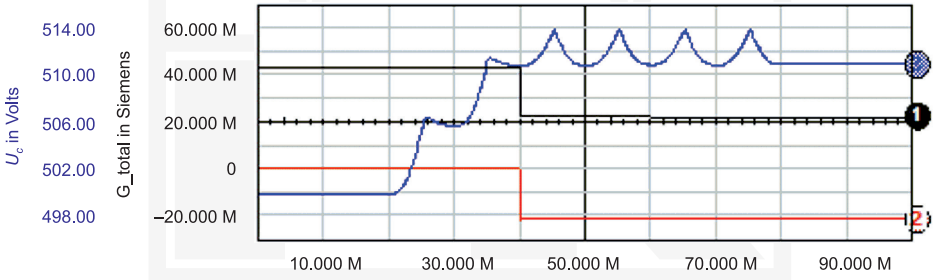

Fig. 7. Filter capacitor voltage (3, blue), and conductance signals: total G (1, black) and variable component ΔG (2, red) – shown in the same scale

Figures 6 and 7 period-table:

0–20 ms: Filter is inactive. Load/source current *RMS* is 8.2 A.

20–40 ms: Filter is active. Source current is determined by G_0 and is greater than load current: *RMS* 10.3 A and 8.2 A, respectively. Filter current *RMS* is 7.2 A. It comprises load non-active current and an excessive active component $(G_0 - G_{2T})u_S$ of source current. Because of this excessive current component, the filter's capacitor voltage rises and the conductance signal on the input terminal of the *S*/*H* element diminishes. That means that in the next period T, the source current will be lowered.

40–60 ms: Corrected magnitude of the equivalent conductance is latched by the *S/H* element at instant t = 40 ms. The variable component ΔG is negative: –20.5 mS. The total conductance and source current are lowered to the accurate magnitudes of 23 mS and *RMS* 6 A, respectively.
60–80 ms: Regular compensation of non-active current.
80–100 ms: Filter is inactive.

The second simulation experiment, Fig. 8, compares source current when using the full reference current formula (12) and then the simplified formula (18). From the figure, it results that these formulae are equivalent to each other.

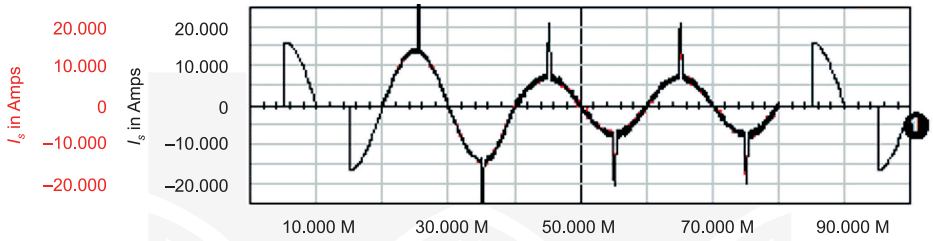

Fig. 8. Source current when full-formula (12) is used (red) and then for simplified formula (18) (black). The red waveform is covered by the black waveform

Third simulation, Figs. 9 and 10: the filter acts without an initial load active power prediction, this means with $G_0 = 0$, see (18).

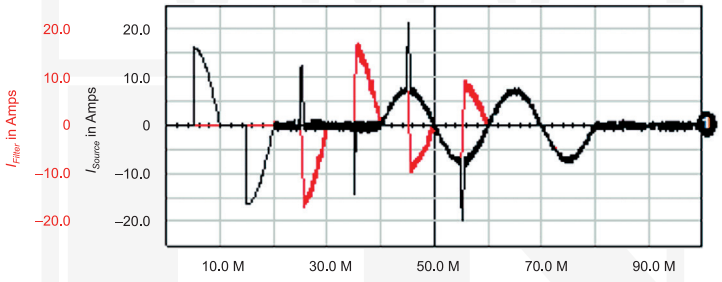

Fig. 9. Source current (black) and filter current (red)

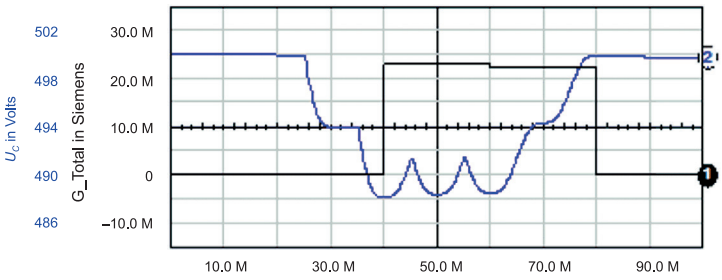

Fig. 10. Load equivalent conductance signal (1) and filter's capacitor voltage (2)

Figures 9 and 10 period-table:
0–20 ms: Filter is off. Load/source current *RMS* is 8.2 A.
20–40 ms: Filter is on. Source current is not flowing due to the conductance condition $G_0 = 0$. Filter current equals load current, i.e. it comprises load active and non-active current components. Filter's capacitor energy diminishes, thus the instantaneous equivalent conductance signal gradually increases.
40–60 ms: The instantaneous equivalent conductance signal is latched at $t = 40$ ms in the *S*/*H* element. The latched signal magnitude is positive and equals 23 mS. Source current *RMS* is 6 A. The filter performs compensation for load non-active current.
60–80 ms: The load is turned off at $t = 60$ ms. However, due to the fact that $G > 0$, the source current is still flowing and charging the filter's capacitor. The capacitor voltage gradually rises to the initial voltage U_{C0}.
80–100 ms: The equivalent conductance signal on the output of the *S*/*H* element falls to zero at the instant when $t = 80$ ms – the source current falls to zero at the same instant. The filter automatically returns to its initial state and is ready to contingent next compensation.

There are a few points which characterise filter action without prediction of initial load active power, this means with $G_0 = 0$:

- The source current is shaped to be active within (0, *T*) time delay.
- The filter's capacitor discharging is a measure of the total equivalent conductance.
- The filter's capacitor acts with lower voltage compared to action with non-zero magnitude of the predefined component G_0.
- After switching the load off, the filter returns to its initial state.

Both modes of filter operation, with or without prediction of initial load active power P_0, are functional and may be used alternatively, dependent upon user requirements.

5. Three-phase filter

Formula (12) may be modified in order to obtain the per-phase active current signal $i^*_{S(k),nT}$ in a three-phase system:

$$i^*_{S(k),nT} = \frac{G_{(n-1)T}}{3} u_{S(k)} \tag{19}$$

$$i^*_{S(k),nT} = \left[\frac{G_0}{3} + \frac{C(U^2_{C0} - U^2_{C,(n-1)T}) + L(I^2_{AF0(k)} - I^2_{AF(k),(n-1)T})}{6TU^2_S} \right] u_{S(k)} \tag{20}$$

where:
$L = L_{FA} = L_{FB} = L_{FC}$
$k = A, B, C.$

After several simplifications, which were described in section 3, equation (20) may be written as:

$$i^*_{S(k),nT} = \left[\frac{G_0}{3} + \alpha_{U\wedge 1}(U_{C0} - U_{C,(n-1)T}) \right] u_{S(k)} \tag{21}$$

Now, the per-phase control structure diagram corresponding with formula (21) may be arranged as is shown in Fig. 11. Voltage signals $u_{S(k)}$ should be provided as positive-sequence fundamental components of respective source phase voltages. A phase-locked-loop system may be used for extracting these components.

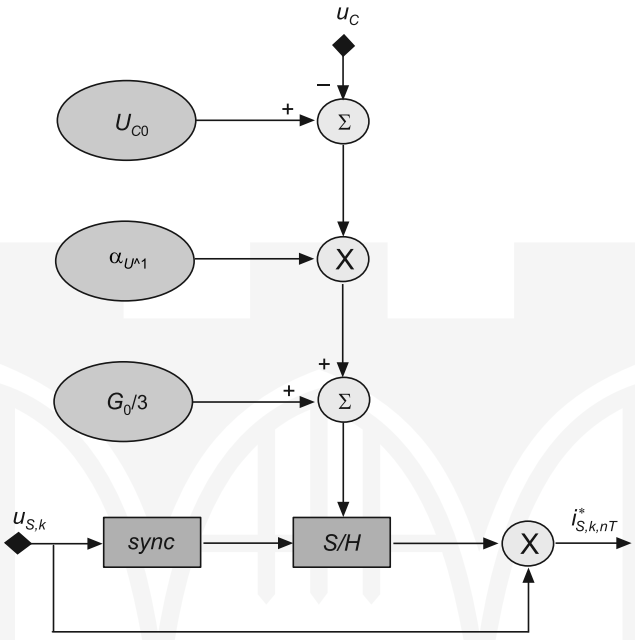

Fig. 11. Per-phase control structure of three-phase active filter

The filter's control circuit shown in Fig. 11 was verified using simulations. Load phase currents were designed to be full of non-active components, especially interharmonics. Such currents are rather impossible in case of a real load, but they are chosen intentionally to show the capability of the active current focused active filter for compensation of complex currents.

Load currents are modelled using three current sources and a time-dependent resistance. Current sources operate in Δ-configuration and generate interharmonics 20 A/60 Hz, 20 A/70 Hz and 25 A/90 Hz in phase *A*, *B*, and *C*, respectively. The time-dependent resistance is connected in parallel with the current source 20 A/60 Hz and changes periodically from zero to 20 Ω with the period 23 ms and duty cycle 11/23. Figure 12 presents load phase currents with source phase voltages. Such a constructed load works asymmetrically. During time period 0–200 ms, source apparent powers are 2350 VA in phase *A*, 2100 VA in phase *B* and 2270 VA in phase *C*. Mean phase powers are 394 W in phase *A*, 403 W in phase *B* and 27 W in phase *C*.

Detection of *DC* components, harmonics, interharmonics and unbalance of such complex signals may be difficult and ambiguous. Note that for the presented control technique, which is focused on active current component only, such load current complexity is not a problem.

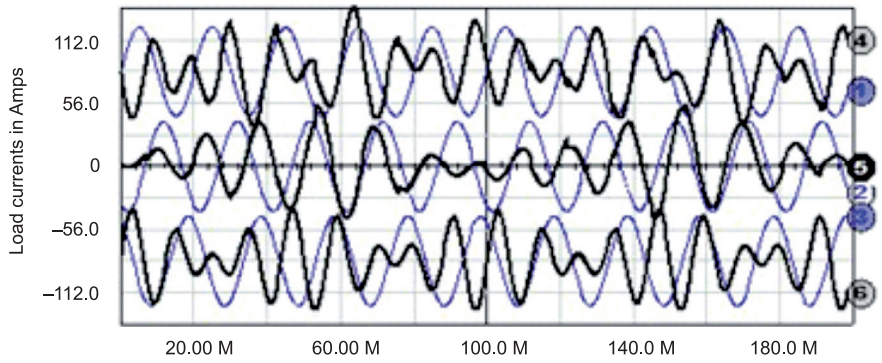

Fig. 12. Load phase currents with source phase voltages

There are two basic methods of bringing successively computed equivalent conductance magnitudes G_{nT} (19) into use:

a) at the same instance for phases *A*, *B*, *C* – for example synchronically with phase voltage of phase *A*, as shown in Fig. 13,
b) successively for phases *A*, *B*, *C* – synchronically with source phase voltages *A*, *B*, *C*, as shown in Fig. 14.

Dependent upon the method used, source currents may be different, but they are sinusoidal within each cycle *T* separately considered, what is shown in Figs. 13–15.

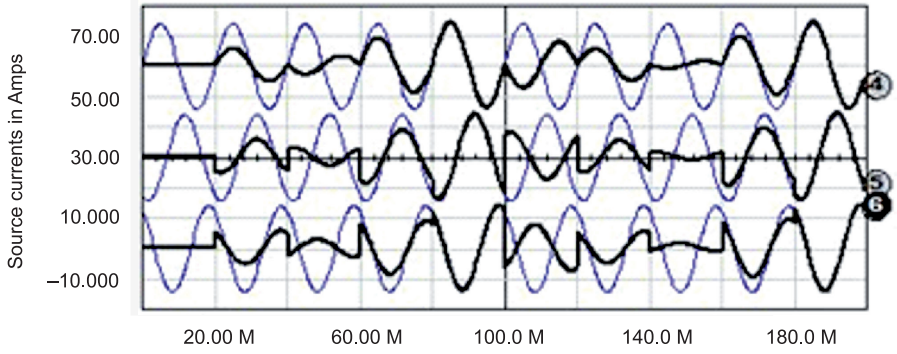

Fig. 13. Source reference currents. Phase currents are synchronised using voltage signal of phase *A*

Dependent upon the method used, source 'power tracks' may also be different due to differences in power buffering: it starts instantly for all phases in method a), or successively in method b). Figure 15 illustrates such an effect showing the filter's capacitor voltage and the equivalent conductance signal G_T for both synchronisation methods. Mean values and standard deviation of the conductance signal are 32 mS and 18 mS for method a); and 23 mS and 53 mS for method b), respectively.

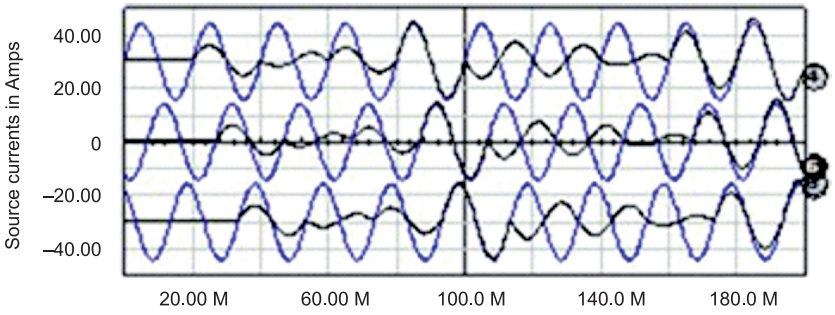

Fig. 14. Source reference currents. Phase currents are synchronised separately, in accordance with corresponding source phase voltage signals

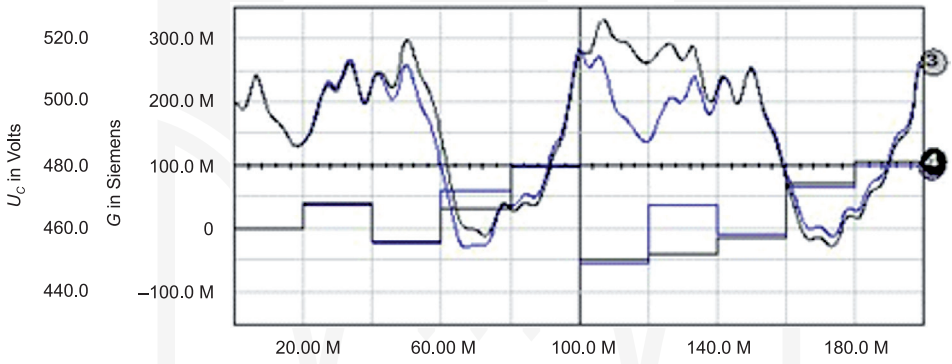

Fig. 15. Comparison of the filter's capacitor voltage and equivalent conductance signal. Synchronisation method a) blue waveforms, method b) black waveforms

For load and source currents shown in Figs. 12–14, *DC* components and amplitudes of current harmonics were obtained by simulation. They were performed separately for some successive *T* periods using the fundamental frequency corresponding to the source voltage cycle. Then, the other set of harmonics was extracted using base frequency of 10 Hz, which is equal to the greatest common divisor of frequencies of the three current sources (60 Hz, 70 Hz and 90 Hz) used to model the load. Fundamental observations can then be highlighted:

1. Source currents *RMS* are significantly reduced. For the time period 0–180 ms, the *RMS* for load phase *A*, *B* and *C* are 23.1 A, 21.0 A and 22.7 A, respectively. For the corresponding time period 20–200 ms, they are 6.2 A for each phase for both synchronisation methods.
2. Source phase currents are in-phase or are in-counter-phase with corresponding phase voltages.
3. Source phase currents are balanced, but *DC* components and current sudden changes may appear in phase *B* and *C* if the load active power changes and if synchronisation method a) is chosen.

4. There are no higher harmonics and *DC* components in source phase currents, but source currents may become unbalanced if the load active power changes and synchronisation method b) is selected.
5. There are significant changes to source current amplitude from one period *T* to another if there are big changes in load active power.

Effects reported in 3–5 above may be reduced if implement controlling of active energy flow. This possibility is considered in section 7.

6. *DC*-system active filter

The active current component is useful by means of carrying the active power. The non--active current component may not only appear in *AC* systems but also in a *DC*-supplied circuit and may be regarded as energetically useless. Hence, compensation may also be advantageous in *DC*-systems. In addition, some new benefits may appear if an energy flow control function implemented in the filter action, see section 7. For example, the life-time of a *DC*-battery depends on the characteristics of the battery's current [33]. If using a properly controlled filter, the battery may work more efficiently and the lifetime of the battery may be increased.

Let us consider an elementary electric circuit consisting of a *DC* voltage source and a varying load. A constant time period *T* may be designated for the circuit. For any *n*-th period *T*, the active power P_{nT} is:

$$P_{nT} = \frac{1}{T}\int_{(n-1)T}^{nT} U_S i_S dt = U_S \frac{1}{T}\int_{(n-1)T}^{nT} i_S dt = U_S I_{Sav,nT} \tag{22}$$

where:

$n = 1, 2, 3, \ldots$; U_S and i_S are source voltage and current,

$I_{Sav,nT}$ – average current in period T_n.

The in-period source current i_{nT} may be split into an active component $i_{p,nT}$ and a non--active component $i_{q,nT}$:

$$i_{nT} = i_{p,nT} + i_{q,nT} \tag{23}$$

The active current is equal to the current average:

$$i_{p,nT} = \frac{P_{nT}}{U_S^2} U_S = \frac{U_S I_{Sav,nT}}{U_S^2} U_S = I_{Sav,nT} \tag{24}$$

This current may be used as the reference for the source current. Using (2)–(13):

$$I^*_{S,nT} = \left[G_0 + \frac{C(U_{C0}^2 - U_{C,(n-1)T}^2) - LI_{AF,(n-1)T}^2}{2TU_S^2} \right] U_S \tag{25}$$

After simplifications (see section 3) equation (25) may be written in the final form:

$$I^*_{S,nT} = \left[G_0 + \alpha_{U\wedge 1}(U_{C0} - U_{C,(n-1)T}) \right] U_S \tag{26}$$

The corresponding structure of the filter control circuit is shown in Fig. 16.

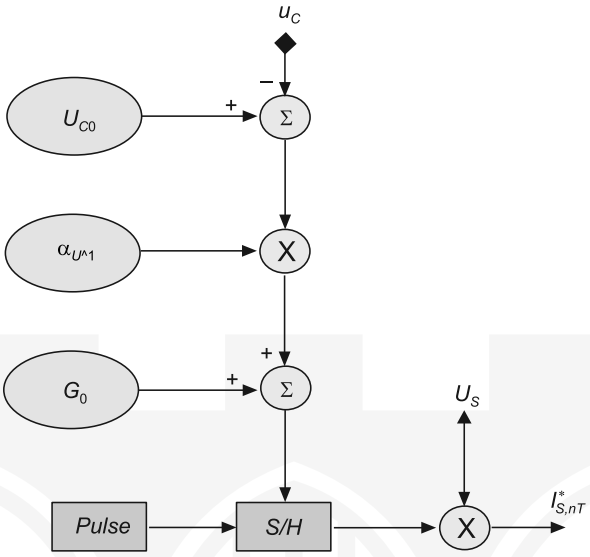

Fig. 16. *DC*-filter control circuit corresponding with (26)

Simulation verification of the considered control method in the *DC*-system was performed. The full-formula (25) and then the simplified formula (26) were examined. The constant component G_0 was set to 80 mS, which is about the mean in the time period 0–100 ms. Figure 17 presents the load current (1, black), the source current (2, green) and the filter current (3, red).

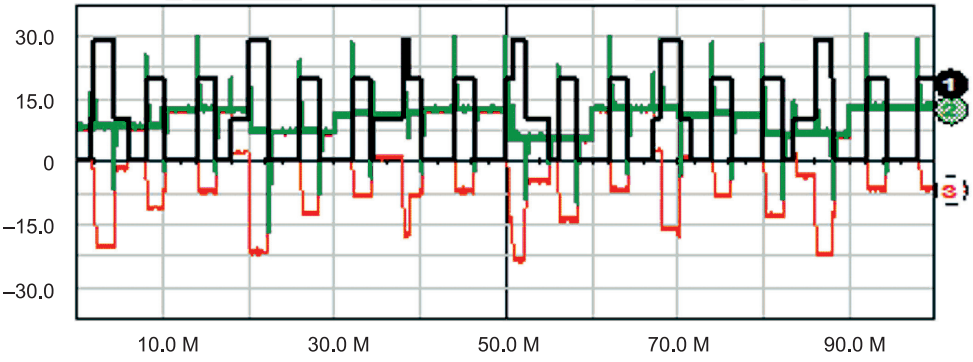

Fig. 17. Load current (1, black), source current (2, green) and filter current (3, red)

The source current *RMS* is significantly reduced. The multi-period load current *RMS* for the time period 0–100 ms is 14.3 A, but the source current within the same time period is diminished to 10.6 A. For the same time, the filter current is 10.8 A.

7. Simultaneous compensation and active energy flow control

As was shown in section 2, the filter acts in a two-step regime. During the first step, the load equivalent conductance is computed and latched, and during the second step, this already time--invariant conductance is used to shape the source current (note, these two steps are performed simultaneously for each cycle of supply voltage). Changes of load active power impacts energy stored in filter's reactance elements. From this perspective, the active filter already buffers some amount of active energy. Such natural mechanism of energy buffering can be developed to build new properties of the active filter. In this paper, two forms of active energy flow regulation are discussed:

a) the *averaging-mode,* which is based on a kind of 'cycle-by-cycle' inertia. In this mode, the filter averages changes of source currents. It virtually converts the actual variable load to be seen as more time-invariant-like,
b) the *storing-mode*. In this mode, the filter can store some amount of energy in its capacitor for future use.

The three-phase circuit with synchronisation by phase *A* is chosen to show features of the filter acting using averaging or storing mode. The load contains the same three current sources operating in the same configuration as described in section 5.

Other filter systems described in the paper were systematically simulated to confirm the usefulness of these two modes of filter operation. The observed filter features were very similar, so there is no need to show these results here.

In order to implement the averaging-mode, the parameter $\alpha_{U^{\wedge}1}$ (21) is reduced to 25% of its nominal magnitude. As a result, *RMS* of source phase reference currents, measured for the time period 20–200 ms, is diminished from 6.2 A to 1.1 A. The filter buffers changes of load active power, hence the source can work more smoothly. Standard deviation of conductance signal G_{nT}, which may be used as a measure of changeability of source active power, is reduced from 48.8 mS to 10.2 mS. Natural versus averaging-mode of filter operation is shown in Fig. 18.

In order to emphasise that the storing-mode is related to energy flow control, the source instantaneous powers are chosen to illustrate features of this mode.

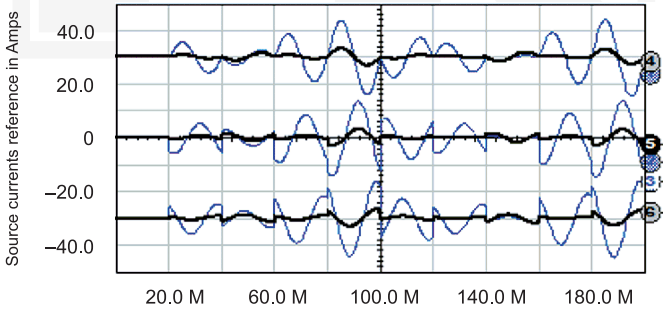

Fig. 18. Phase source currents for the natural and then for the averaging-mode. Synchronization method a) is applied. Phase currents *RMS* are reduced from 6.2 A (blue waveforms) to 1.1 A (black waveforms)

Before switching the active filter on the source phase, instantaneous powers are non--sinusoidal and non-periodical. Additionally, during the load work there are T periods when the load consumes energy, and there are other periods when the load generates energy. As a result, the total instantaneous source power is also highly irregular, Fig. 19.

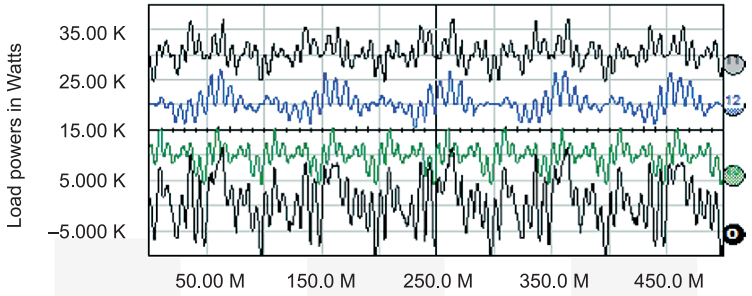

Fig. 19. Source instantaneous powers in phase A, B, C and total power as the sum of phase powers. There is no active filter action yet

After the active filter is switched on, source phase currents become sinusoidal and balanced, so phase instantaneous powers become sinusoidal and balanced and the source total instantaneous power becomes constant within each voltage cycle, Fig. 20.

In the example, there are time periods when the load generates energy. Note, generated powers are different for each load phase, Fig. 19. If implementing the storing-mode, this energy can be stored in the filter's capacitor for future use without sending it to the source. In the storing-mode, the active filter persistently compensates for the non-active phase current components and acts simultaneously as a local energy accumulator. In order to store the 'from-load' energy in the filter, negative magnitudes of the conductance signal G_{nT} are blocked. As a result, all source instantaneous powers have only positive magnitudes, Fig. 20.

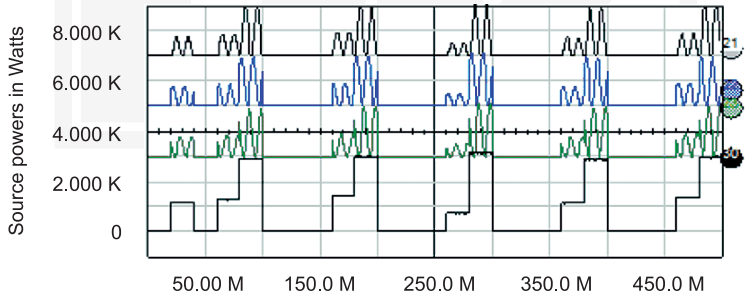

Fig. 20. Source instantaneous powers in phase A, B, C and source total power. Storing-mode is used

Unfortunately, the source works in a pulsing-like way. Standard deviation of the equivalent conductance signal may be a measure of such a disadvantageous pulsation. In the example, the standard deviation and the mean of the conductance are 38.9 mS and

29.4 mS, respectively. This pulsation may be alleviated if combining the storing-mode with the averaging-mode. In order to add the averaging-mode to the filter action, the parameter $\alpha_{U\wedge 1}$ (21) was reduced to 25% of its nominal magnitude. As a result, the standard deviation and the mean of the conductance are reduced to 12.6 mS and 23.4 mS, respectively. Source powers are shown in Fig. 21.

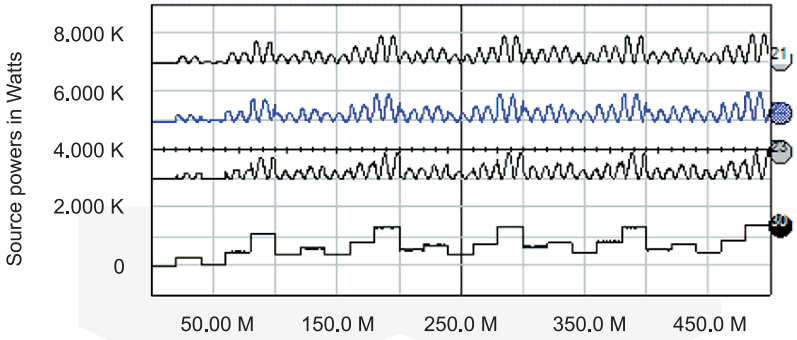

Fig. 21. Source instantaneous powers in phase *A*, *B*, *C* and total power. Storing-mode and averaging-mode are applied concurrently

8. Universality of filter's control method

The considered filter is as universal in its control algorithm as in its hardware structure. The same filter arrangement may be used in *DC*, single-phase and three-phase system for the following reasons:

a) the load equivalent conductance is always determined using energy stored in the filter's capacitor. Hence the same form of function of the filter's capacitor voltage may be utilized to obtain the reference current,
b) the common hardware structure utilises the three-leg inverter. If using the filter in single-phase or in *DC*-system, the filter can act as a two-leg subsystem of the whole device, see Fig. 22.

In addition, if utilising the Current Source Inverter based active filter, equation (10) is still valid. Equations similar to (18), (21) and (26) may be written, respectively, as:

$$i^*_{S,nT} = \left[G_0 + \alpha_{I\wedge 1}(\mathrm{I}_{L0} - I_{L,(n-1)T}) \right] u_S \tag{27}$$

or

$$i^*_{S(k),nT} = \left[\frac{G_0}{3} + \alpha_{I\wedge 1}(I_{L0} - I_{L,(n-1)T}) \right] u_{S(k)} \tag{28}$$

or

$$i^*_{S,nT} = \left[G_0 + \alpha_{I\wedge 1}(\mathrm{I}_{L0} - I_{L,(n-1)T}) \right] U_S \tag{29}$$

Structures shown in Figs. 5, 11 and 16 are also valid if replacing the initial capacitor voltage U_{C0} for the initial filter's *DC*-side inductor current constant I_{L0}.

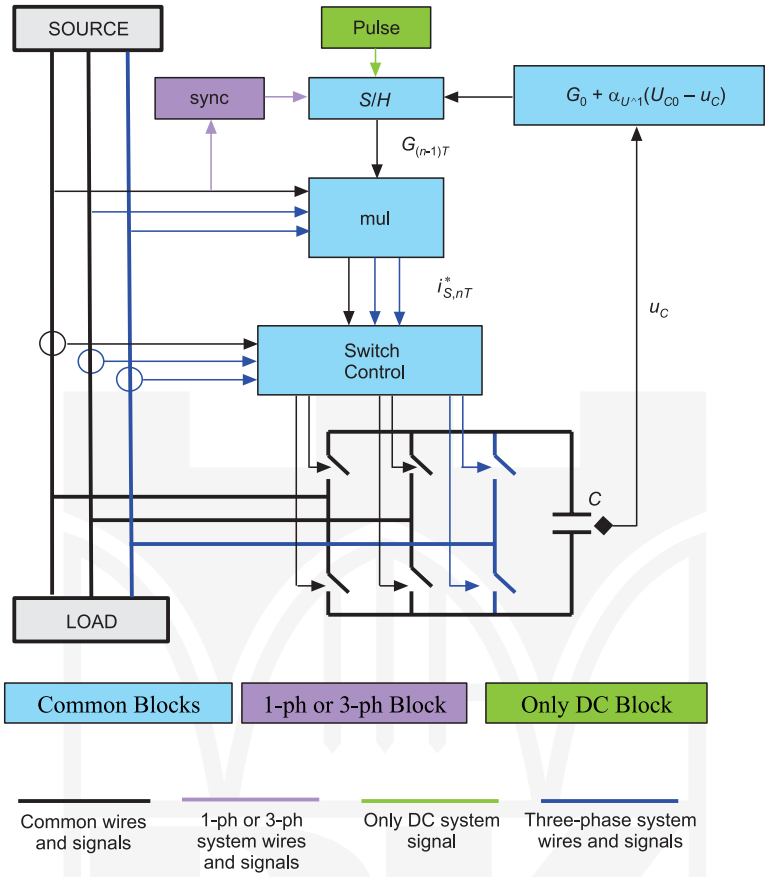

Fig. 22. Universal filter structure

9. Conclusion

Certain changes of energy stored in the active filter's reactance elements may be utilised as the source of information concerning the load active current component. This component can then be used as the reference signal for compensation. After analysis, it turned out that this energy-based control method may be substituted with the simplified strategy, which is based on measuring and simple processing of the filter's capacitor *DC*-side voltage or the filter's inductor *DC*-side current. The described control method allows using the filter not only to compensate the non-active current but, additionally, to buffer the bi-directional flow of active energy between the source and compensated loads. In such a case, the filter acts simultaneously as a local energy accumulator. The control algorithm is universal and may be employed in *DC*, single-phase and three-phase active filters.

References

[1] Asiminoaei L., Blaabjerg F., Hansen S., *Detection is key. Harmonic detection methods for active power filter applications*, IEEE Ind. Appl. Mag., 2007, Vol. 13(4), 22-33.

[2] Miret J., Castilla M., Mattas J., Guerrero J.M., Vasquez J.C., *Selective harmonic-compensation control for single-phase active power filter with high harmonic rejection*, IEEE Trans. on Ind. Electr., 2009, Vol. 56(8), 3117-3127.

[3] Mariethoz S., Rufer A.C., *Open loop and closed loop spectral frequency active filtering*, IEEE Trans on Pow. Electr., 2002, Vol. 17(4), 564-573.

[4] Rahmani S., Al-Haddad K., Fnaiech Y., *Comparison of two PWM techniques for a single-phase shunt active power filter applying indirect current control*, IEEE Int. Conf. on Ind. Techn., 2004, 639-644.

[5] Farrokhi M., Jamali S., Mousavi S.A., *Fuzzy logic based indirect current control of the shunt active power filter*, IEEE Univ. Pow. Eng. Conf., 2004, 489-493.

[6] Singh B.N., Singh B., Chandra A., Rastgoufard P., Al-Haddad K., *An improved control algorithm for active filter*, IEEE Trans. on Power Delivery, 2007, Vol. 22(2), 1009-1020.

[7] Nedeljković D., Nemec M., Drobnić K., Ambrožić V., *Direct current control of active power filter without filter current measurement*, Int. Symp. on Pow. Electron., Electr. Drives, Aut. and Mot., 2008, 72-76.

[8] Khadkikar V., Chandra A., Singh B.N., *Generalised single-phase p-q theory for active power filtering: simulation and DSP-based experimental investigation*, IET Pow. Electron., 2009, Vol. 2(1), 67-78.

[9] Orts-Grau S., Gimeno-Sales F.J., Segui-Chilet S., Abellen-Garcia A., Alcaniz-Fillol M., Masot--Peris R., *Selective compensation in four-wire electric systems based on a new equivalent conductance approach*, IEEE Trans. on Ind. Electr., 2009, Vol. 56(8), 2862-2874.

[10] Vardar K., Akpinar E., *Comparing ADALINE and IRPT methods based on shunt active power filter*, Euro. Trans. Electr. Power, 2011, Vol. 21, 924-936.

[11] Wu J.-C., Jou H.-L., *Simplified control method for the single-phase active power filter*, IEE Proc.--Electr. Power Appl., 1996, Vol. 143(3), 219-224.

[12] Tang Y., Loh P.C., Wang P., Choo F.H., Gao F., Blaabjerg F., *Generalized Design of High Performance Shunt Active Power Filter With Output LCL Filter*, IEEE Trans. on Ind. Electr., 2012, Vol. 59(3), 1443-1452.

[13] Piróg S., *PWM rectifier and active filter with sliding-mode control*, EPE Trondheim, 1997.

[14] Singh B.N., Chandra A., Al-Haddad K., *Performance comparison of two control techniques applied to an active filter*, Int. Conf. on Harm. and Qual. of Power, 1, 1998, 133-138.

[15] Huang S.-J., Wu J.-C., *A control algorithm for three-phase three-wired active power filters under nonideal mains voltages*, IEEE Trans. on Power Electr., 1999, Vol. 14(4), 753-760.

[16] Chandra A., Singh B., Singh B.N., Al-Haddad K., *An improved control algorithm of shunt active filter for voltage regulation, harmonic elimination, power-factor correction, and balancing of nonlinear loads*, IEEE Trans. on Ind. Electr., 2000, Vol. 15(3), 495-507.

[17] Azevedo H.J., Ferreira J.M., Martins A.P., Carvalho A.S., *Direct current control of an active power filter for harmonic elimination, power factor correction and load unbalancing compensation*, EPE, Toulouse 2003.

[18] Nunez-Zuniga T.E., Pomilio J.A., *Shunt active power filter synthesizing resistive loads*, IEEE Trans. on Ind. Electr., 2002, Vol. 17(2), 273-278.

[19] Hamadi A., Al-Haddad K., Lagace P.J., Chandra A., *Indirect current control techniques of three-phase APF using fuzzy logic and proportional integral controller: Comparative analysis*, Int. Conf. on Harm. and Qual. of Power, 2004, 362-367.

[20] Singh B.N., *Sliding mode control technique for indirect current controlled active filter*, IEEE Annual Reg. 5 Conf., 2003, 51-58.
[21] Strzelecki R., Benysek G., Jarnut M., *Power quality conditioners with minimum number of current sensor requirement*, Int. School on Nonsin. Currents and Compensation, 2008, 1-4.
[22] Watson R.V., *Sampled energy control of a single-phase shunt active power filter synthesizing a resistive load*, EPE 2009.
[23] Chen Z., Luo Y., Chen M., Shi L., Li J., *Design and implementation of a high performance aeronautical active power filter*, IEEE Ann. Conf. IECON, 2010, 2032-2037.
[24] Fei J., Li T., Zhang S., *Indirect current control of active filter using novel sliding mode controller*, Workshop on Control and Modeling for Power Electronics, 2012, 1-6.
[25] Szromba A., *A shunt active power filter: development of properties*, COMPEL, 2004, Vol. 23(2), 735-46.
[26] Szromba A., *Energy controlled shunt active power filters*, COMPEL, 2007, Vol. 26(4), 1142--1160.
[27] Szromba A., *Sampled Method of Active Power Filter Control (Part I)*, Electric. Pow. Quality and Utilisation J., 2005, Vol. 11(2), 91-98.
[28] Szromba A., *Sampled Method of Active Power Filter Control (Part II)*, Electric. Pow. Quality and Utilisation J., 2006, Vol. 12(1), 16-25.
[29] Bhattacharya A., Chakraborty C., *A Shunt Active Power Filter With Enhanced Performance Using ANN-Based Predictive and Adaptive Controllers*, IEEE Trans. on Ind. Electr., 2011, Vol. 58(2), 421-428.
[30] Hwang J.-G., Park Y.-J., Choi G.-H., *Indirect current control of active filter for harmonic elimination with novel observer-based noise reduction scheme*, Electric. Engineering, 2005, Vol. 87, 261-266.
[31] Fryze S., *Wirk-, Blind-, und Scheinleistung in Elektrischen Stromkreisen mit nichtsinusformigem Verlauf von Strom und Spannung.*, ETZ 53, 1932, 596-599, 625-627, 700-702.
[32] Moreno V., Pigazo A., *Modified FBD method in active power filters to minimize the line current harmonics*, IEEE Trans. on Pow. Deliv., 2007, Vol. 22(1), 735-746.
[33] Savoye F., Venet P., Millet M., Groot J., *Impact of periodic current pulse on Li-Ion battery performance*, IEEE Trans. on Ind. Electr., 2012, Vol. 59(9), 3481-3488.